Supplementary information

Title:

Identifying the global and transcallosal layer-specific connectivity with bilateral line-scanning fMRI

Headline:

Interhemispheric layer-specific line-scanning fMRI

Authors:

Sangcheon Choi[1,2] , Yi Chen[2], Hang Zeng[2,3], Bharat Biswal[4], Xin Yu[1,*]

Affiliations:

1 Athinoula A. Martinos Center for Biomedical Imaging, Department of Radiology, Harvard Medical School, Massachusetts General Hospital, Charlestown, MA 02129, USA

2 Max Planck Institute for Biological Cybernetics, Tübingen 72076, Baden-Württemberg, Germany

3 Graduate Training Centre of Neuroscience, University of Tübingen, Tübingen 72076, Baden-Württemberg, Germany

4 Department of Biomedical Engineering, NJIT, Newark, NJ 07102, USA

Supplementary Table: 1

Supplementary Figures: 11

***Lead corresponding author:**

Dr. Xin Yu

Email: xyu9@mgh.harvard.edu, Telephone: 617 626 3197

Address: 13th Street, Charlestown, MA 02129, USA

Table S1. Details of animals and trials for BiLS acquisition.

Animal #	Total	Evoked			Resting-state		
1	16	Trial #	Meas #	Delays (min)	Trial #	Meas #	Delays (min)
		1	29	229.9*	1	44	244.1*
		2	48	62.5	2	47	33.4
		3	52	11.7	3	48	15.0
		4	54	27.2	4	51	58.0
		5	56	26.3	5	55	54.1
		6	58	24.2	6	57	15.0
		7	60	25.4	7	61	50.2
		8	62	26.0	8	63	25.2
2	13	Trial #	Meas #	Delays (min)	Trial #	Meas #	Delays (min)
		1	21	170.0*	1	25	183.8*
		2	26	36.5	2	27	23.1
		3	28	26.4	3	29	44.1
		4	48	295.0	4	32	24.6
		5	56	123.4	5	34	25.1
					6	46	184.3
					7	49	44.3
					8	52	73.7
3	24	Trial #	Meas #	Delays (min)	Trial #	Meas #	Delays (min)
		1	35	264.5*	1	24	100.9*
		2	39	50.9	2	25	14.3
		3	41	27.7	3	27	21.9
		4	46	61.4	4	29	30.1
		5	47	13.6	5	30	11.8
		6	48	12.6	6	36	99.6
		7	50	24.6	7	38	24.8
		8	52	27.2	8	40	23.8
		9	54	25.1	9	42	27.9
					10	43	12.1

					11	44	12.3
					12	45	12.2
					13	49	51.0
					14	51	27.9
					15	53	25.0
4	2	Trial #	Meas #	Delays (min)	Trial #	Meas #	Delays (min)
		1	39	245.1*	1	40	258.2*
5	12	Trial #	Meas #	Delays (min)	Trial #	Meas #	Delays (min)
		1	31	64.9*	1	30	43.2*
		2	32	15.8	2	33	50.4
		3	34	24.3	3	35	28.3
		4	36	28.4	4	37	24.4
		5	38	23.8	5	39	24.0
		6	40	24.2	6	41	24.4
6	10	Trial #	Meas #	Delays (min)	Trial #	Meas #	Delays (min)
		1	22	60.3*	1	24	95.9*
		2	25	47.2	2	26	24.5
		3	27	24.8	3	28	24.8
		4	29	24.3	4	30	24.0
		5	32	37.6	5	33	44.2
Total #	77	34			43		

The delay (*) of the first trial each animal was calculated as difference from the first MRI acquisition (*e.g.*, Tripilot). To verify evoked fMRI responses between measurements, a few 3D GRE-EPI (3 min) and 2D bSSFP (6 min) images were acquired. For animal #3 and #4, rs-fMRI has more trials than evoked fMRI because some of evoked trials didn't have BOLD responses upon stimulation.

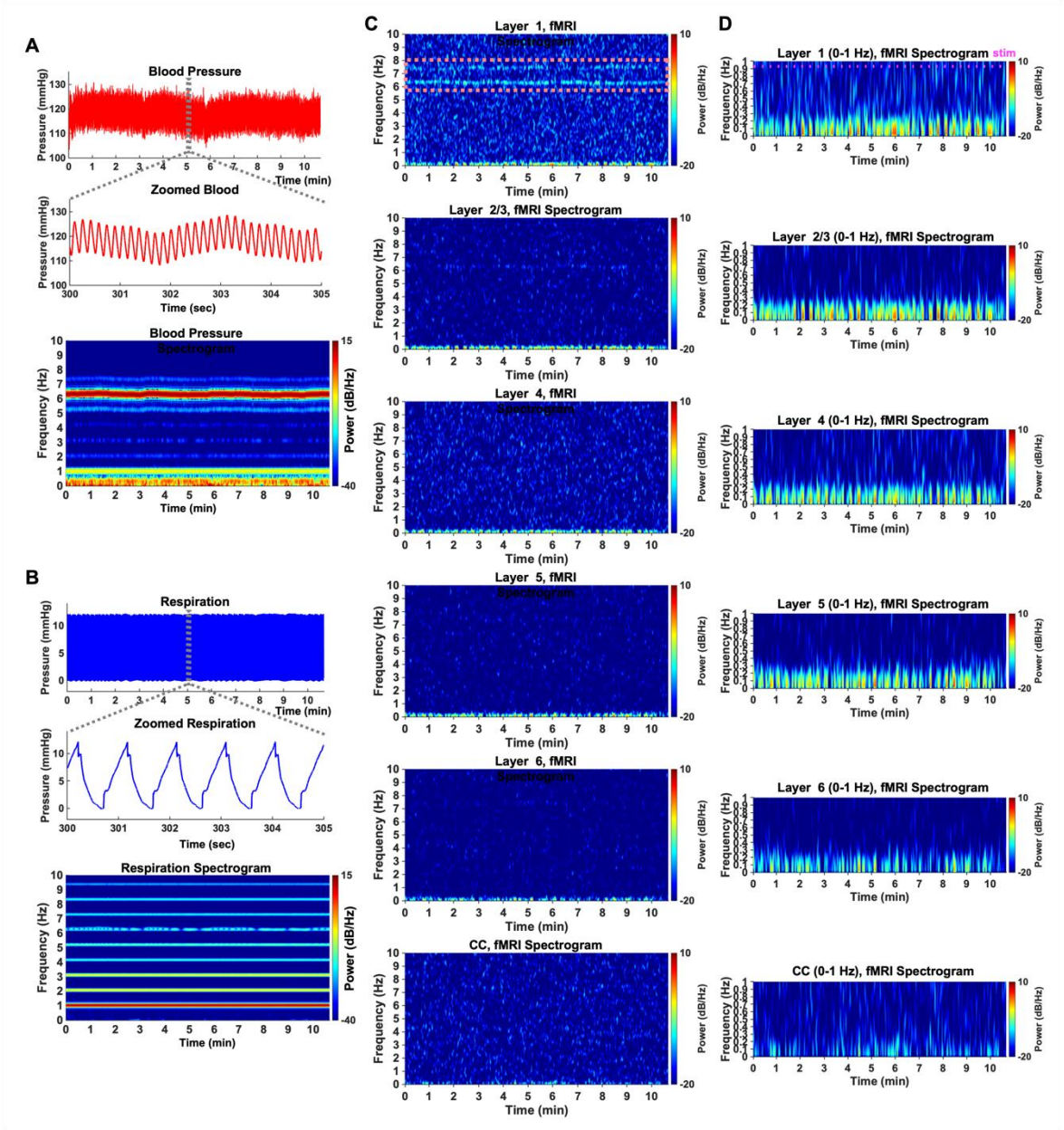

Figure S1. Effect of cardiorespiratory noises on laminar-specific evoked fMRI signals from a representative trial (TR 50

ms). **A**. *Top*: Arterial blood pressure time courses. *Middle:* Zoomed time courses from the upper time course (gray box). *Bottom:* The blood pressure spectrogram showing 5-8 Hz cardiac cycle. **B**. *Top*: Respiration time courses. *Middle:* Zoomed time courses from the upper time course (gray box). *Bottom:* The respiration spectrogram showing 1 Hz respiratory cycle and its harmonics. **C**. Layer-wise fMRI spectrograms from L1 to CC (from top to bottom) to show aliasing artifacts of the cardiorespiratory noises (magenta box) in the individual layers. **D**. Zoomed layer-wise fMRI spectrograms which show that no cardiorespiratory aliasing effects exist on evoked fMRI responses (0-1 Hz).

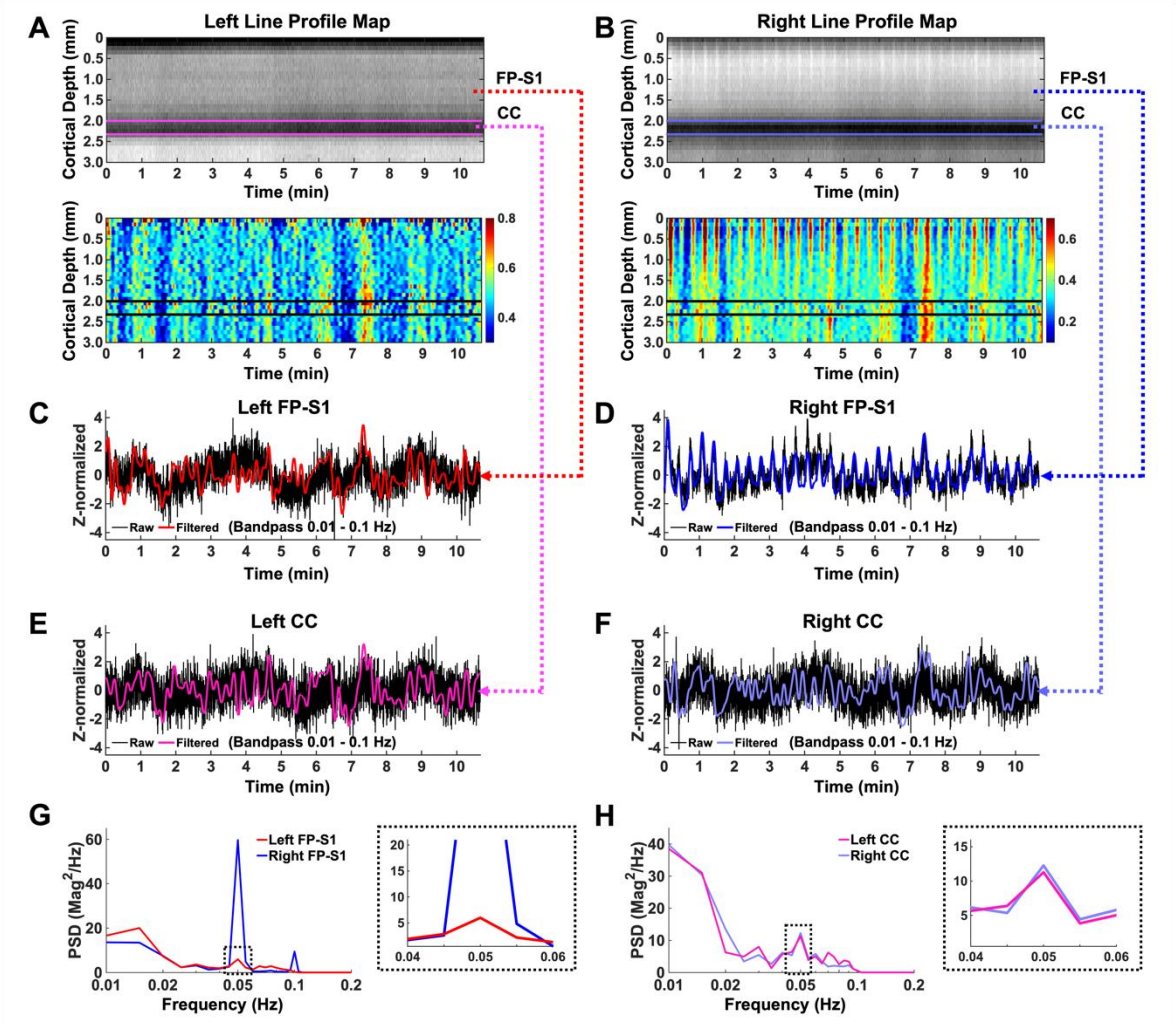

Figure S2. Evoked fMRI time series and BOLD responses in bilateral FP-S1 and corpus callosum regions from a representative trial. **A** and **B.** *Top*: Spatiotemporal maps consist of bilateral line-scanning profiles which were concatenated for 32 epochs (10 min 40 sec) from the left and right FP-S1 (0-2 mm), the left and right CC (2.0-2.3 mm) between the magenta lines and between the light purple lines respectively. *Bottom*: Normalized spatiotemporal maps show the laminar-specific responses in cortex and CC responses for the same regions as the upper images. The black lines indicate the left

and right CC regions, the same as the magenta and light purple lines of the top images. **C** and **D.** The Z-score normalized fMRI time series of raw (black) and filtered (red and blue) data (average of 20 voxels, bandpass: 0.01-0.1 Hz) in the left and right FP-S1 during electrical stimulation to the left forepaw (block design: 1 s pre-stim, 4 s stim, and 15 s post-stim). **E** and **F.** The Z-score normalized fMRI time series of raw (black) and filtered (magenta and light purple) data (average of 20 voxels, bandpass: 0.01-0.1 Hz) in the left and right CC with the same period as **C** and **D**. **G** and **H.** The power spectral densities (PSDs) of the filtered and Z-score normalized fMRI time series from the left (red) and right (blue) FP-S1 (**G**), left (magenta) and right (light purple) CC regions (**H**) clearly show the evoked frequency responses (0.05 Hz) with enlarged PSDs (0.04-0.06 Hz, dashed black box).

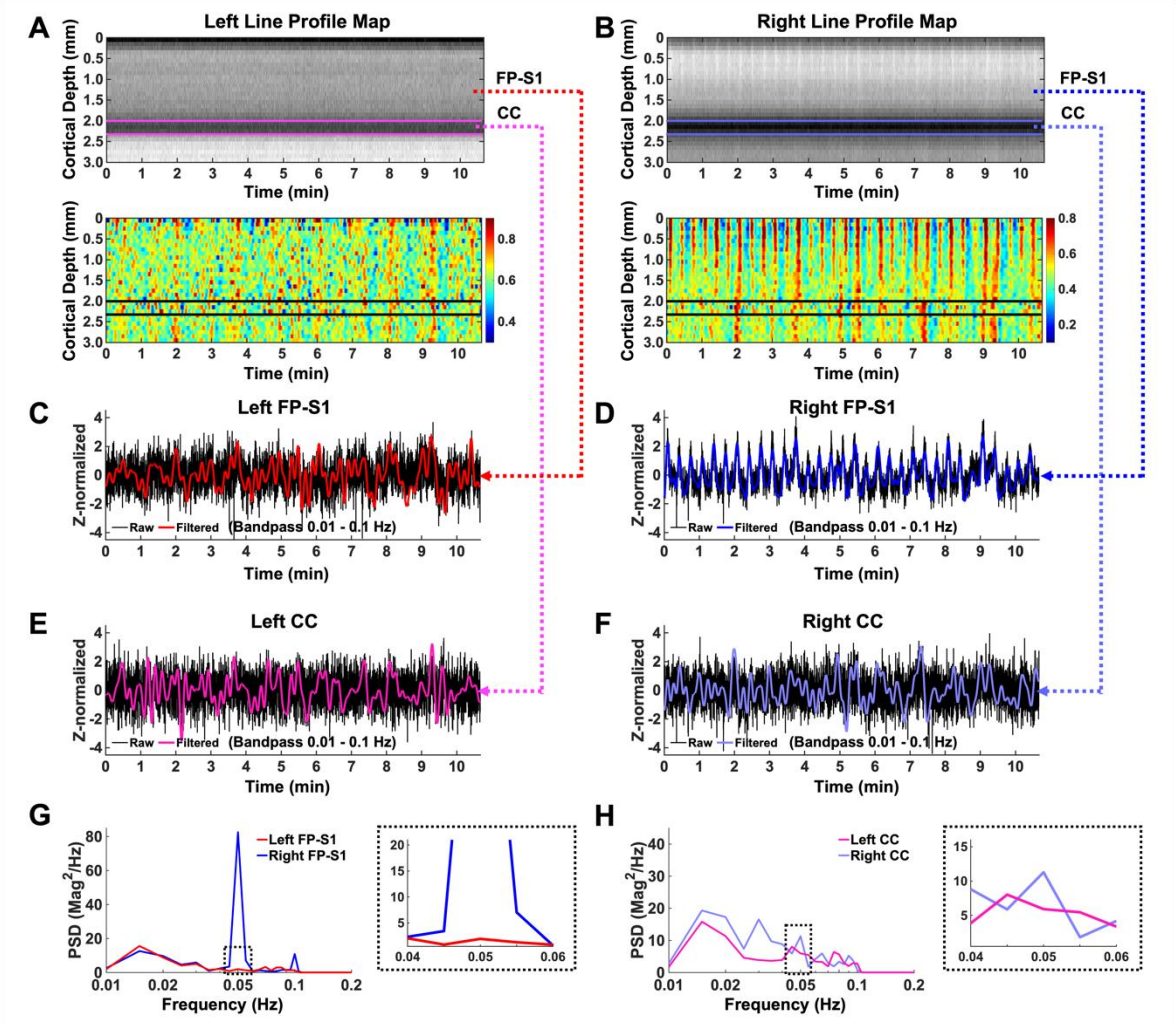

Figure S3. Evoked fMRI time series and BOLD responses in bilateral FP-S1 and CC from one representative trial (absence of CC activation). **A** and **B**. *Top*: Spatiotemporal maps consist of bilateral line-scanning profiles which were concatenated for 32 epochs (10 min 40 sec) from the left (red) and right (blue) FP-S1 (0-2 mm), the left and right CC (2.0-2.3 mm) between the magenta lines and between the light purple lines respectively. *Bottom*: Normalized spatiotemporal maps show the laminar-specific responses in the cortex and CC responses for the same regions as the upper images. The black lines

indicate the left and right corpus callosum regions, the same as the magenta and light purple lines of the top images. **C** and **D**. The Z-score normalized fMRI time series of raw (black) and filtered (red and blue) data (average of 20 voxels, bandpass: 0.01-0.1 Hz) in the left and right FP-S1 regions during electrical stimulation to the left forepaw (block design: 1 s pre-stim, 4 s stim, and 15 s post-stim, 32 epochs, 10 min 40 sec). **E** and **F**. The Z-score normalized fMRI time series of raw (black) and filtered (magenta and light purple) data (average of 20 voxels, bandpass: 0.01-0.1 Hz) in the left and right CC regions during the same period as **C** and **D**. **G** and **H**. The power spectral densities (PSDs) of the filtered and Z-score normalized fMRI time series show the evoked frequency responses (0.05 Hz) with enlarged PSDs (0.04-0.06 Hz, dashed black box) from the left (red) and right (blue) FP-S1 (**G**). No local peak exists at evoked frequency responses (0.05 Hz) in the left CC (**H**, magenta line).

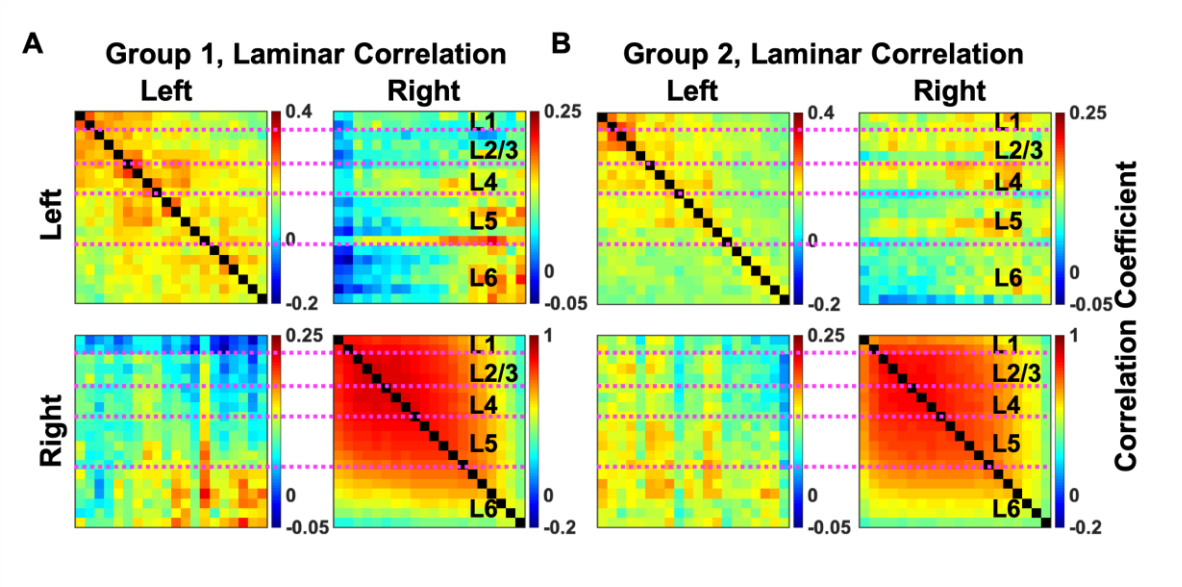

Figure S4. Group-averaged results representing laminar-specific correlation across the layers (L1, L2/3, L4, L5, L6) in Group 1 (**A**) and Group 2 (**B**). **A**. Group 1 shows negative correlations between superficial layers (L1) of right FP-S1 and all layers of left FP-S1. **B**. Group 2 only shows positive correlations between infragranular layers of right FP-S1 (L5 and 6) and all layers of left FP-S1.

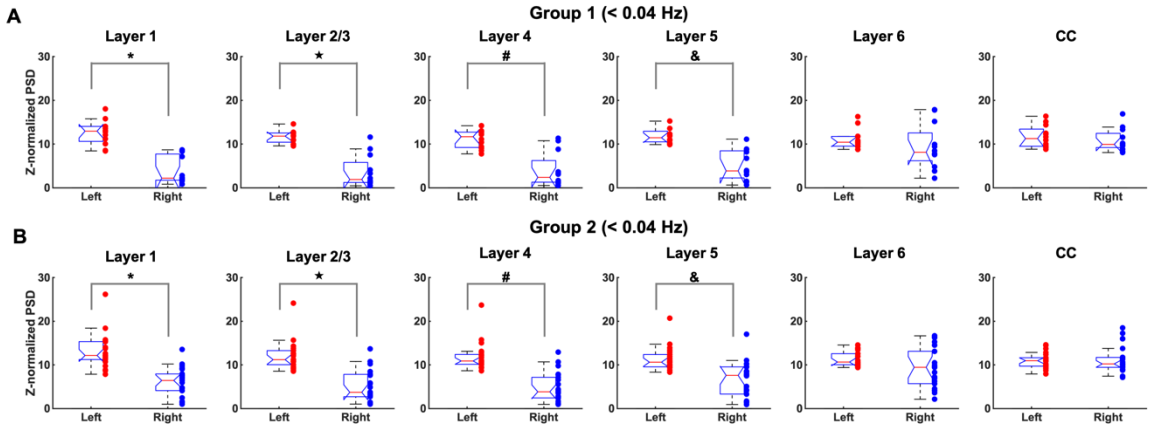

Figure S5. Comparison of Z-normalized PSDs of ultra-slow oscillation (<0.04 Hz) at all the layers (L1-6) and CC in the left (red) and right (blue) FP-S1 of Group 1 (**A**) and 2 (**B**). Individual symbols from L1-4 represent significant difference between the left and right layers (Student t-test: $^{\star, \blacktriangle, \#, \&}p < 0.05$). Layer 6 and CC show no significant difference between the left and right sides.

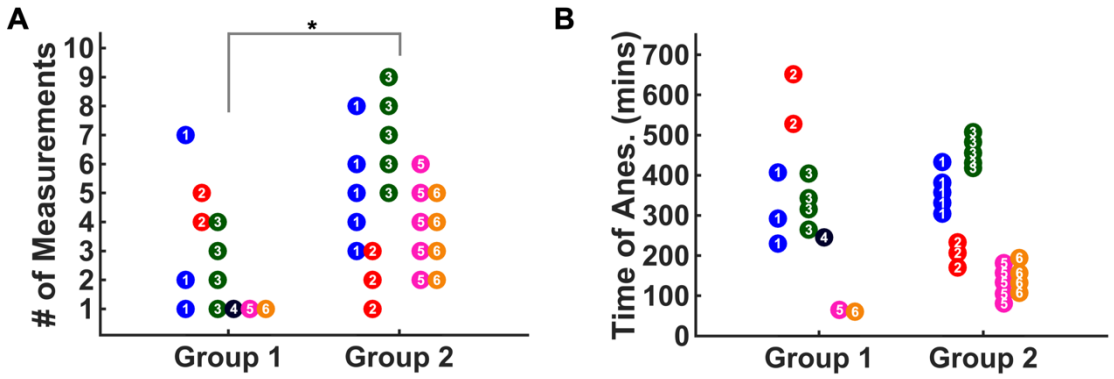

Figure S6. Dependency on the number of measurements and the time of anesthesia for assigning trials of either group 1 or 2 (6 animals, 34 trials). Numbers indicate individual animals and colors indicate data points from the same animal. **A.** Scatter plots for the number of measurements in Group 1 and 2. The number of measurements between two groups shows significant difference (independent group t-test, $p^* = 0.01593$). **B.** Scatter plots for the time of anesthesia in Group 1 and 2 . The time of anesthesia between two groups shows no significant difference ($p = 0.40101$). The correlation of the number of measurements and the time of anesthesia in each group were highly correlated (Group 1: 0.7586, Group 2: 0.7902).

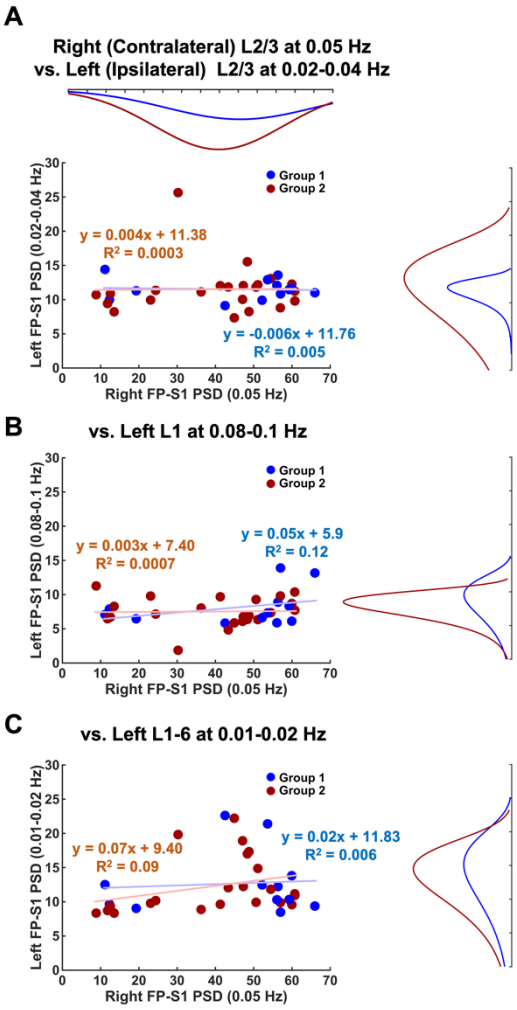

Figure S7. Comparison between Right (contralateral) FP-S1 (L2/3) responses at 0.05 Hz to left (ipsilateral) FP-S1 activity at 0.02-0.04Hz (L2/3), 0.08-0.1Hz (L1), and 0.01-0.02Hz across all layers. **A-C.** Scatter plots of Z-normalized PSDs in the right L2/3 at 0.05 Hz vs. the left L2/3 at 0.02-0.04 Hz (**A**), vs. the left L1 at 0.08-0.1 Hz (**B**), vs. the left L1-6 at 0.08-0.1 Hz (**C**). Individual dots represent trials (n = 34) and histogram fitting plots show distribution of the PSD values of Group 1 (blue) and 2 (brown). linear plots indicate 1st-order fitting lines to the data of Group 1 (blue) and 2 (red).

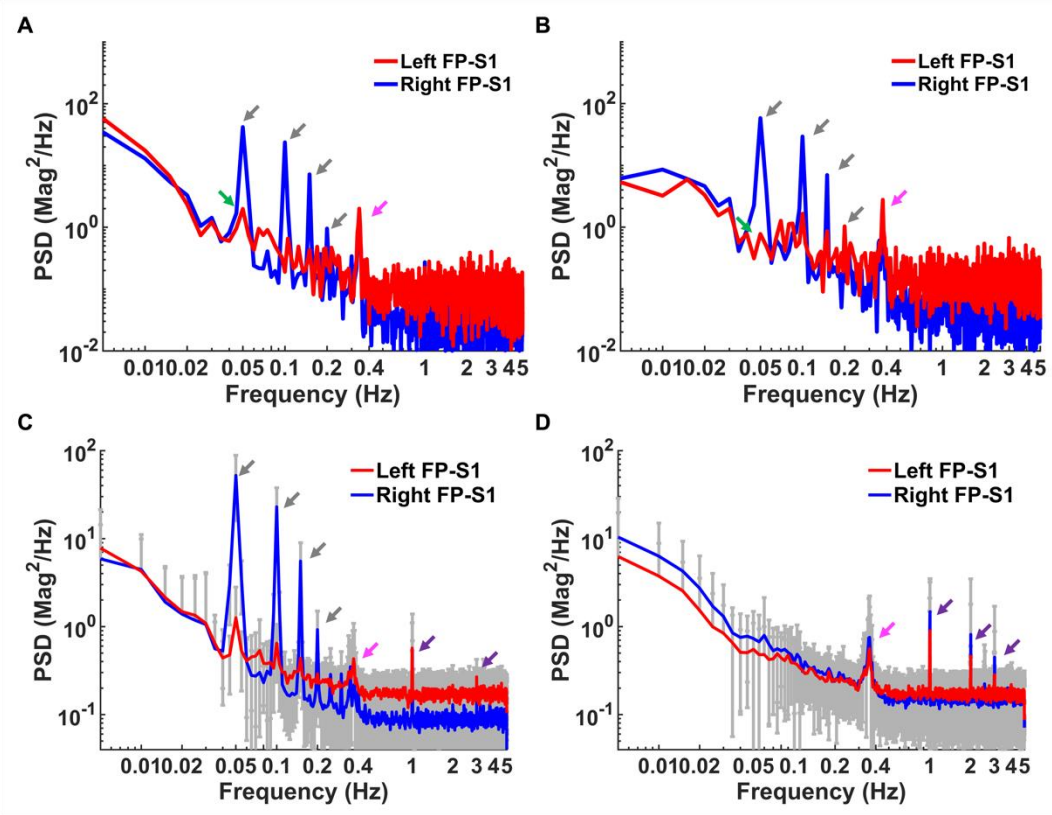

Figure S8. Power spectral densities from 0.01 to 5 Hz (Nyquist frequency) in evoked (**A-C**) and rs-fMRI (**D**). **A-D.** Bilateral abrupt PSD peaks appear at 0.3 - 0.4 Hz (magenta arrows) in both evoked and rs-fMRI. **A-B.** Evoked responses in the left (ipsilateral) FP-S1 (green arrows) and the right (contralateral) FP-S1 (gray arrows) from one representative evoked trial of Group 1 (**A**, **Fig. S2**) and another representative evoked trial of Group 2 (**B**, **Fig. S3**). **C-D.** Averaged bilateral PSDs exhibit stimulation frequency responses and its harmonics in evoked fMRI (**C**, gray arrows), which were void of resting-state frequency responses (**D**). Distinct respiratory peaks and its harmonics appeared at 1 Hz and subsequent frequencies (purple arrows). Error bars represent mean ± SD across 6 animals.

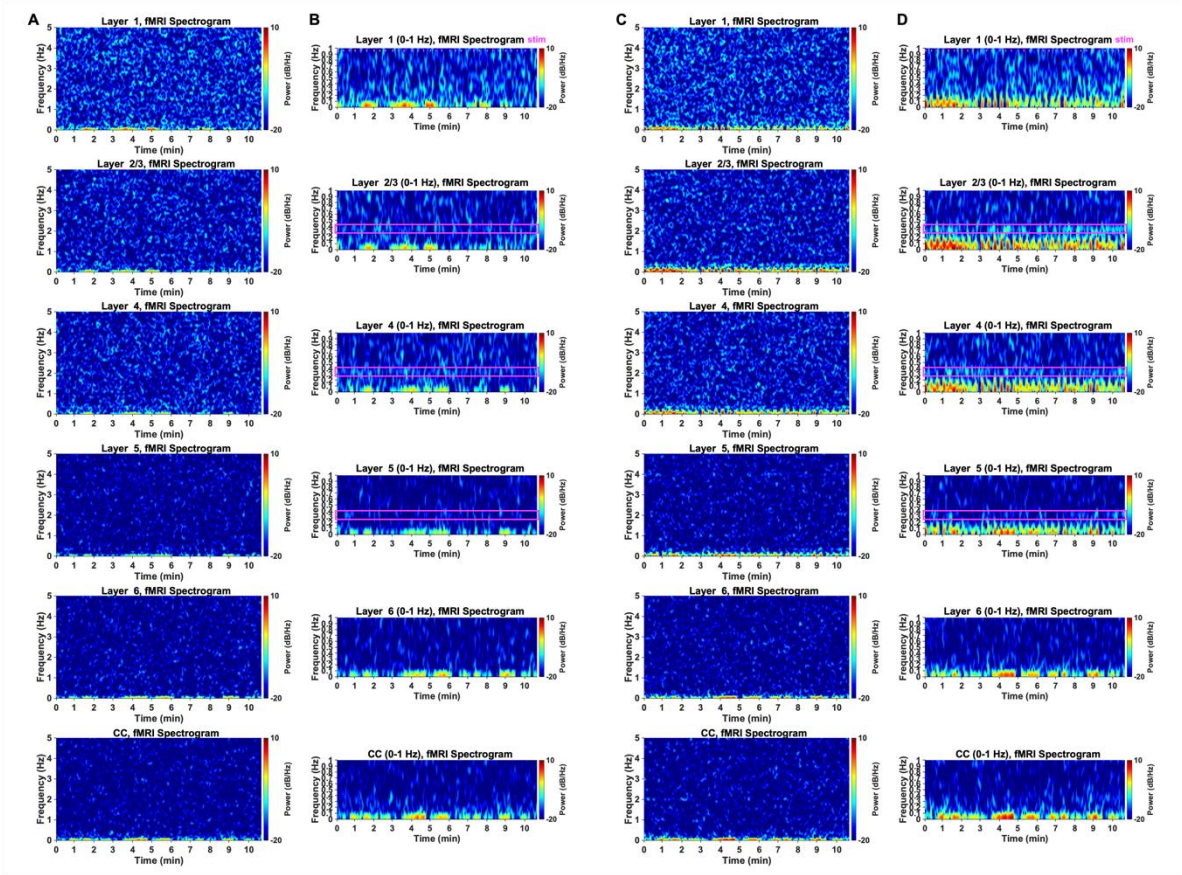

Figure S9. Power spectrograms of laminar-specific evoked fMRI signals from a representative trial (**Fig. S2**) of Group 1 in evoked fMRI. **A** and **C**. Layer-wise fMRI spectrograms from L1 to CC (from top to bottom) to show time-frequency responses from 0 to 5 Hz (Nyquist sampling frequency) in the individual layers of left (**A**) and right (**C**) FP-S1. **B**-**D**. Zoomed layer-wise fMRI spectrograms which show that Mayer waves at ~ 0.3-0.4 Hz exist in both FP-S1 regions (magenta box).

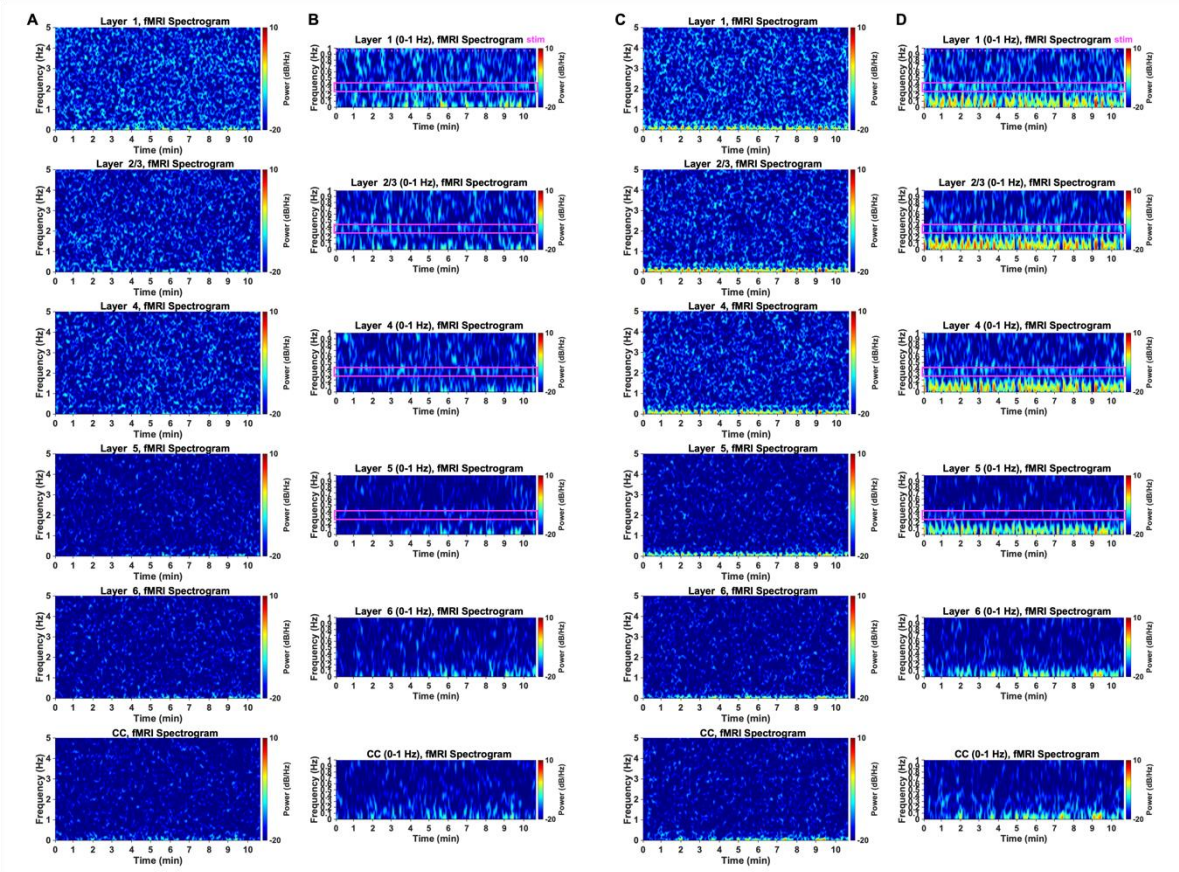

Figure S10. Power spectrograms of laminar-specific evoked fMRI signals from one representative trial (**Fig. S3**) of Group 2 in evoked fMRI. **A** and **C**. Layer-wise fMRI spectrograms from L1 to CC (from top to bottom) to show time-frequency responses from 0 to 5 Hz (Nyquist sampling frequency) in the individual layers of left (**A**) and right (**C**) FP-S1. **B-D**. Zoomed layer-wise fMRI spectrograms which show that Mayer waves at ~ 0.3-0.4 Hz exist in both FP-S1 regions (magenta box).

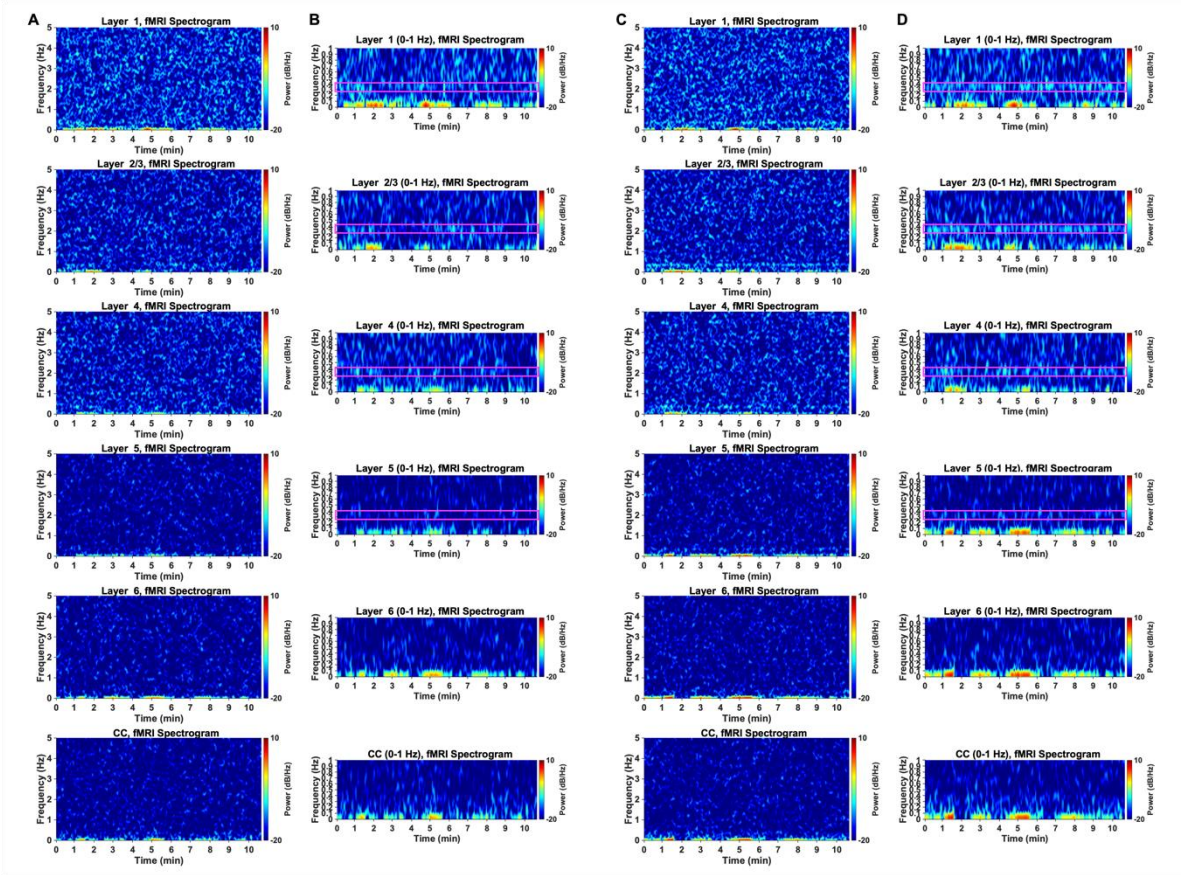

Figure S11. Power spectrograms of laminar-specific evoked fMRI signals from one representative trial (**Fig. 3A** and **B**) in rs-fMRI. **A** and **C**. Layer-wise fMRI spectrograms from L1 to CC (from top to bottom) to show time-frequency responses from 0 to 5 Hz (Nyquist sampling frequency) in the individual layers of left (**A**) and right (**C**) FP-S1. **B**-**D**. Zoomed layer-wise fMRI spectrograms which show that Mayer waves at ~ 0.3-0.4 Hz exist in both FP-S1 regions (magenta box).